Supporting Information

Binary Targeting of siRNA to Hematologic Cancer Cells *In Vivo* using Layer-by-Layer Nanoparticles

Ki Young Choi[1,2,3], Santiago Correa[1,4], Jouha Min[1,2], Jiahe Li[1,2], Sweta Roy[1], Kristiana H Laccetti[1], Erik Dreaden[1,2], Stephanie Kong[1,2], Roun Heo[5], Young Hoon Roh[1,2,6], Edward C Lawson[7], Peter A Palmer[7], and Paula T Hammond[1,2]

[1] Koch Institute for Integrative Cancer Research, Massachusetts Institute of Technology, Cambridge, MA, 02139, USA

[2] Department of Chemical Engineering, Massachusetts Institute of Technology, Cambridge, MA, 02139, USA

[3] Natural Product Informatics Research Center, Korea Institute of Science and Technology, Gangneung 25451, Republic of Korea.

[4] Materials Science and Engineering, Stanford University, Palo Alto, CA, 94305, USA

[5] Department of Health Sciences and Technology, SAIHST, Sungkyunkwan University, Suwon 440-746, Republic of Korea.

[6] Department of Biotechnology, Yonsei University, Seoul, 120-749, Republic of Korea.

[7] Janssen Research and Development, LLC, Spring House, PA, 19477, USA

Correspondence should be addressed to P.T.H. (hammond@mit.edu)

Supporting Table S1. BCL-2 siRNA Cocktail Sequences

BCL-2 siRNA cocktail (Target NCBI gene ID: 596)	
Sense sequence	**Antisense sequence**
GAGGATTGTGGCCTTCTTT	AAAGAAGGCCACAATCCTC
GGGAGAACAGGGTACGATA	TATCGTACCCTGTTCTCCC
CCACCTGTGGTCCACCTGA	TCAGGTGGACCACAGGTGG
CCCTGTGGATGACTGAGTA	TACTCAGTCATCCACAGGG
GGCGCACGCTGGGAGAACA	TGTTCTCCCAGCGTGCGCC
GCCGCGACTTCGCCGAGAT	ATCTCGGCGAAGTCGCGGC
CTGCACCTGACGCCCTTCA	TGAAGGGCGTCAGGTGCAG
CGAGTGGGATGCGGGAGAT	ATCTCCCGCATCCCACTCG
GAGATAGTGATGAAGTACA	TGTACTTCATCACTATCTC
GGGTACGATAACCGGGAGA	TCTCCCGGTTATCGTACCC
CGGTGCCACCTGTGGTCCA	TGGACCACAGGTGGCACCG
GTGATGAAGTACATCCATT	AATGGATGTACTTCATCAC
GGCCTTCTTTGAGTTCGGT	ACCGAACTCAAAGAAGGCC
GGGAGGATTGTGGCCTTCT	AGAAGGCCACAATCCTCCC
GGATGACTGAGTACCTGAA	TTCAGGTACTCAGTCATCC
GTACGATAACCGGGAGATA	TATCTCCCGGTTATCGTAC
CGCGACTTCGCCGAGATGT	ACATCTCGGCGAAGTCGCG
CCCGCACCGGGCATCTTCT	AGAAGATGCCCGGTGCGGG
GTGGACAACATCGCCCTGT	ACAGGGCGATGTTGTCCAC
CAGGCCGGCGACGACTTCT	AGAAGTCGTCGCCGGCCTG
GGGCCACAAGTGAAGTCAA	TTGACTTCACTTGTGGCCC
GGCTCGCTCAATCAAGAAA	TTTCTTGATTGAGCGAGCC
GCCTATACACTATTTGTGA	TCACAAATAGTGTATAGGC
GCATACCTGGTGGGAGGAA	TTCCTCCCACCAGGTATGC
GTGCTGCTATCCTGCCAAA	TTTGGCAGGATAGCAGCAC
GGGCCCTCCAGATAGCTCA	TGAGCTATCTGGAGGGCCC
GCATTGAAGTGAGGTGTCA	TGACACCTCACTTCAATGC
GGATGTTCTGTGCCTGTAA	TTACAGGCACAGAACATCC
GGATACTTTACATGGTTAA	TTAACCATGTAAAGTATCC
GAATTGGAGAGTGATAATA	TATTATCACTCTCCAATTC
GGGAACTATAAAGAAGTAA	TTACTTCTTTATAGTTCCC
CATGAGATTCATTCAGTTA	TAACTGAATGAATCTCATG
CCGCATTTAATTCATGGTA	TACCATGAATTAAATGCGG
GGGCTGTGATATTAACAGA	TCTGTTAATATCACAGCCC
GCCCAGACAAATGTGGTTA	TAACCACATTTGTCTGGGC
GAGTGAACAGAATTGCAAA	TTTGCAATTCTGTTCACTC
GAAGGACAGCGATGGGAAA	TTTCCCATCGCTGTCCTTC
CTGTGGCATTATTGCATTA	TAATGCAATAATGCCACAG
GGCTCTGTCTGAGTAAGAA	TTCTTACTCAGACAGAGCC
CCATCGGGTCGTCTCCGAA	TTCGGAGACGACCCGATGG

Supporting Table S2. GAPDH siRNA Cocktail Sequences

GAPDH siRNA cocktail (Target NCBI gene ID: 2597)	
Sense sequence	**Antisense sequence**
GATGCCCCCATGTTCGTCA	TGACGAACATGGGGGCATC
GCGATGCTGGCGCTGAGTA	TACTCAGCGCCAGCATCGC
GACAACAGCCTCAAGATCA	TGATCTTGAGGCTGTTGTC
CCTGCCAAATATGATGACA	TGTCATCATATTTGGCAGG
GGGGCTCTCCAGAACATCA	TGATGTTCTGGAGAGCCCC
CCCCACTGCCAACGTGTCA	TGACACGTTGGCAGTGGGG
CCACCCAGAAGACTGTGGA	TCCACAGTCTTCTGGGTGG
GGAGCCAAAAGGGTCATCA	TGATGACCCTTTTGGCTCC
GGAGTCCCTGCCACACTCA	TGAGTGTGGCAGGGACTCC
CAGCAAGAGCACAAGAGGA	TCCTCTTGTGCTCTTGCTG
GCACCGTCAAGGCTGAGAA	TTCTCAGCCTTGACGGTGC
CAACTTTGGTATCGTGGAA	TTCCACGATACCAAAGTTG
GAATTTGGCTACAGCAACA	TGTTGCTGTAGCCAAATTC
GCATTGCCCTCAACGACCA	TGGTCGTTGAGGGCAATGC
GAAGCTTGTCATCAATGGA	TCCATTGATGACAAGCTTC
CATGGCCTCCAAGGAGTAA	TTACTCCTTGGAGGCCATG
CTCAACGACCACTTTGTCA	TGACAAAGTGGTCGTTGAG
CTGCACCACCAACTGCTTA	TAAGCAGTTGGTGGTGCAG
CCCACTCCTCCACCTTTGA	TCAAAGGTGGAGGAGTGGG
GTGGTCTCCTCTGACTTCA	TGAAGTCAGAGGAGACCAC
CATGTAGACCCCTTGAAGA	TCTTCAAGGGGTCTACATG
CTCACAGTTGCCATGTAGA	TCTACATGGCAACTGTGAG
CATGAGAAGTATGACAACA	TGTTGTCATACTTCTCATG
CTCATTTCCTGGTATGACA	TGTCATACCAGGAAATGAG
CGCACCTTGTCATGTACCA	TGGTACATGACAAGGTGCG
GTGTGAACCATGAGAAGTA	TACTTCTCATGGTTCACAC
CTGACCTGCCGTCTAGAAA	TTTCTAGACGGCAGGTCAG
CCACCCATGGCAAATTCCA	TGGAATTTGCCATGGGTGG
CGAGATCCCTCCAAAATCA	TGATTTTGGAGGGATCTCG
GTCATGTACCATCAATAAA	TTTATTGATGGTACATGAC
GATGCCCCCATGTTCGTCA	TGACGAACATGGGGGCATC
GCGATGCTGGCGCTGAGTA	TACTCAGCGCCAGCATCGC
GACAACAGCCTCAAGATCA	TGATCTTGAGGCTGTTGTC
CCTGCCAAATATGATGACA	TGTCATCATATTTGGCAGG

Supporting Table S3. Negative Control siRNA Cocktail Sequences

Negative control siRNA cocktail	
Sense sequence	**Antisense sequence**
TGTACGCGTCTCGCGATTT	AAATCGCGAGACGCGTACA
TATACGCGGTACGATCGTT	AACGATCGTACCGCGTATA
TTCGCGTAATAGCGATCGT	ACGATCGCTATTACGCGAA
TCGGCGTAGTTTCGACGAT	ATCGTCGAAACTACGCCGA
TCGCGTAAGGTTCGCGTAT	ATACGCGAACCTTACGCGA
TCGCGATTTTAGCGCGTAT	ATACGCGCTAAAATCGCGA
TCGCGTATATACGCTACGT	ACGTAGCGTATATACGCGA
TTTCGCGAACGCGCGTAAT	ATTACGCGCGTTCGCGAAA
TCGTATCGTATCGTACCGT	ACGGTACGATACGATACGA
TTATCGCGCGTTATCGCGT	ACGCGATAACGCGCGATAA
TCTCGTAGGTACGCGATCT	AGATCGCGTACCTACGAGA
TCGTACTCGATAGCGCAAT	ATTGCGCTATCGAGTACGA
TTTGCGATACCGTAACGCT	AGCGTTACGGTATCGCAAA
TGCGTAAGGCATGTCGTAT	ATACGACATGCCTTACGCA
TTATCGGCAGTTCGCCGTT	AACGGCGAACTGCCGATAA
TAGCGCGACATCTATCGCT	AGCGATAGATGTCGCGCTA
TCGTCGTATCAGCGCGTTT	AAACGCGCTGATACGACGA
TACGCGAAACTGCGTTCGT	ACGAACGCAGTTTCGCGTA
TCGACGATAGCTATCGCGT	ACGCGATAGCTATCGTCGA
TCGCGTAATACGCGATCGT	ACGATCGCGTATTACGCGA
TCGCGATAATGTTACGCGT	ACGCGTAACATTATCGCGA
TTAACGCGCTACGCGTATT	AATACGCGTAGCGCGTTAA
TCGCGTATAGGTAACGCGT	ACGCGTTACCTATACGCGA
TTACGCGATCACGTAACGT	ACGTTACGTGATCGCGTAA
TTATCGCGCGTCGCGTAAT	ATTACGCGACGCGCGATAA
TTACGTACTAGTGCGTACT	AGTACGCACTAGTACGTAA
TATACGCCGGTTGCGTAGT	ACTACGCAACCGGCGTATA
TTCGCGTGCATAGCGTAAT	ATTACGCTATGCACGCGAA
TACGCGACCTAATCGCGAT	ATCGCGATTAGGTCGCGTA
TCGTACGCTGAACGCGTAT	ATACGCGTTCAGCGTACGA

Supporting Table S4. BCL-2 Target Single siRNA Sequences

BCL-2 siRNA1	
Sense sequence	**Antisense sequence**
UUUCCUGCAUCUCAUGCCA	UGGCAUGAGAUGCAGGAAA
BCL-2 siRNA2	
Sense sequence	**Antisense sequence**
CAGGACCUCGCCGCUGCAGAC	CGGUCCUGGAGCGGCGACGUCUG

Supporting Table S5. Off-Target Effects of BCL-2 target siRNAs

Sample	Off target gene	Tscan score	Expression (%)	SD
siRNA1	PHF10	-0.938	76.096	5.116
	MRPL48	-0.778	90.685	11.302
	EFNA4	-0.775	91.833	4.768
	VAMP5	-0.734	121.455	16.646
	CCNB1IP1	-0.71	102.412	25.332
	SSFA2	-0.7	60.769	3.354
	NUPL2	-0.686	79	17.706
	OSMR	-0.667	111.556	10.116
	MTA3	-0.652	98.297	12.366
	SDHD	-0.643	49.375	6.272
siRNA2	HIST1H2BK	-0.709	29.365	2.354
	ZG16B	-0.703	88.738	9.883
	TTC32	-0.695	88.38	4.806
	NDUFA11	-0.664	22.944	1.668
	ATPIF1	-0.656	76.237	12.684
Cocktail	NDUFB2	-1.038	118.133	18.361
	SMIM20	-1.036	135.965	15.403
	SRP9	-1.026	74.652	16.239
	NDUFB5	-1.003	94.021	46.2
	CCNO	-0.971	84.435	12.57
	PPCS	-0.95	96.67	19.007
	NUDT3	-0.927	71.402	9.069

TargetScan Score. TargetScan gives scores ranging from -2 to 0 to indicate the off-target risk for individual genes. -2 is the strongest indication, which however still only gives a 40% accuracy (i.e. more than 50% of the predictions could be wrong). For scores of -1, the accuracy drops below 10% (i.e. >90% of the off-target predictions could be wrong).

Lysine modification

❑Step 1: Polyelectrolyte modification

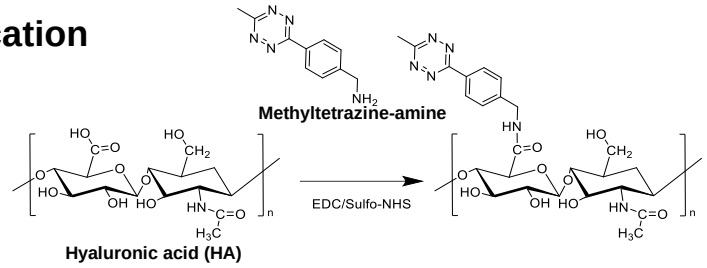

❑Step 2: Anti-CD20 antibody modification

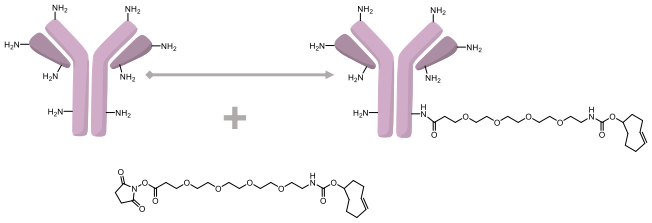

❑Step 3: NP modification

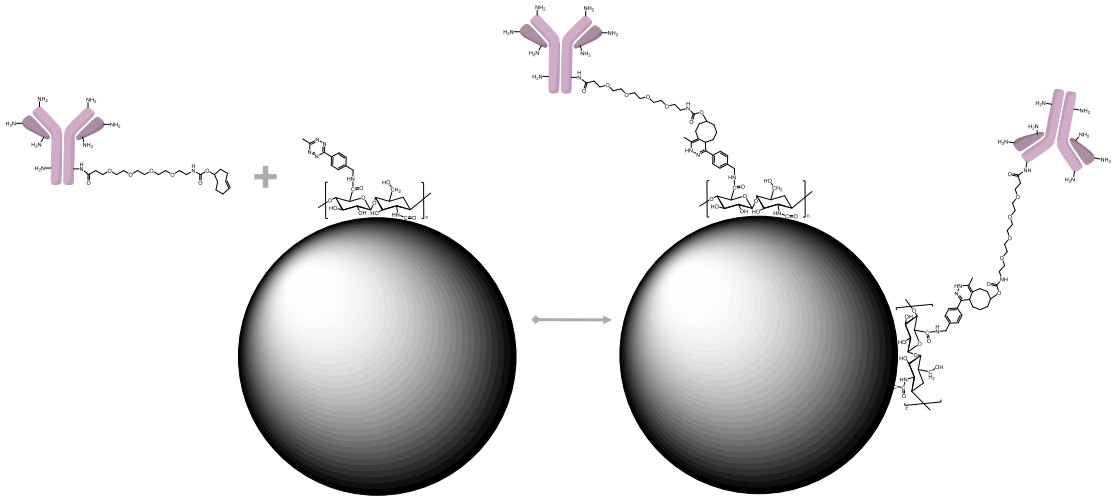

Supporting Information Scheme S1. Schematic illustration of lysine modification steps for preparation of LbLTCO-modified anti-CD20 antibody.

Sulfhydryl modification

❑Step 1: Polyelectrolyte modification

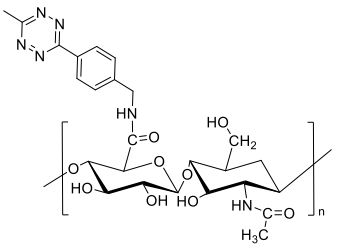

❑Step 2: Ab modification

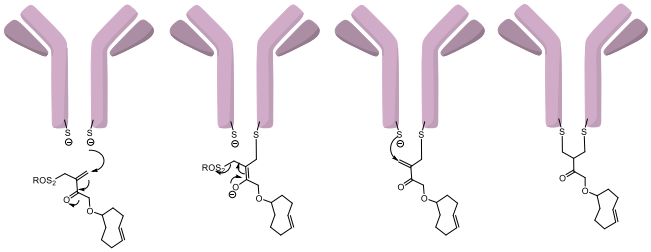

❑Step 3: NP modification

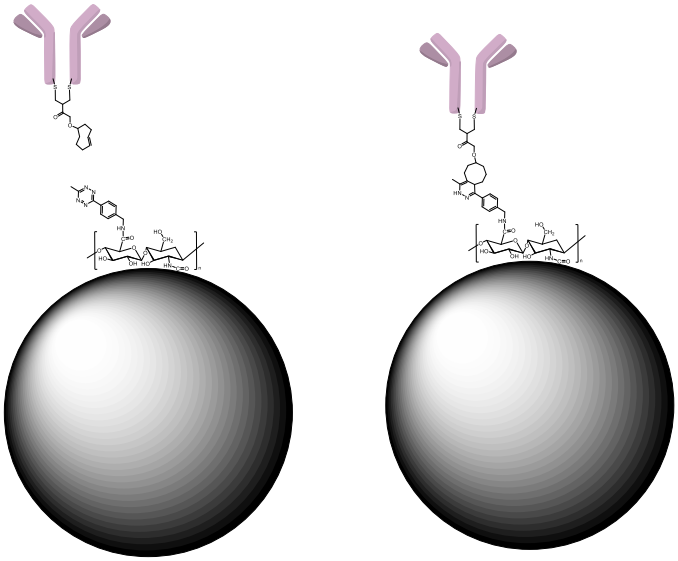

Supporting Information Scheme S2. Schematic illustration of sulfhydryl modification steps for preparation of TCO-modified anti-CD20 antibody.

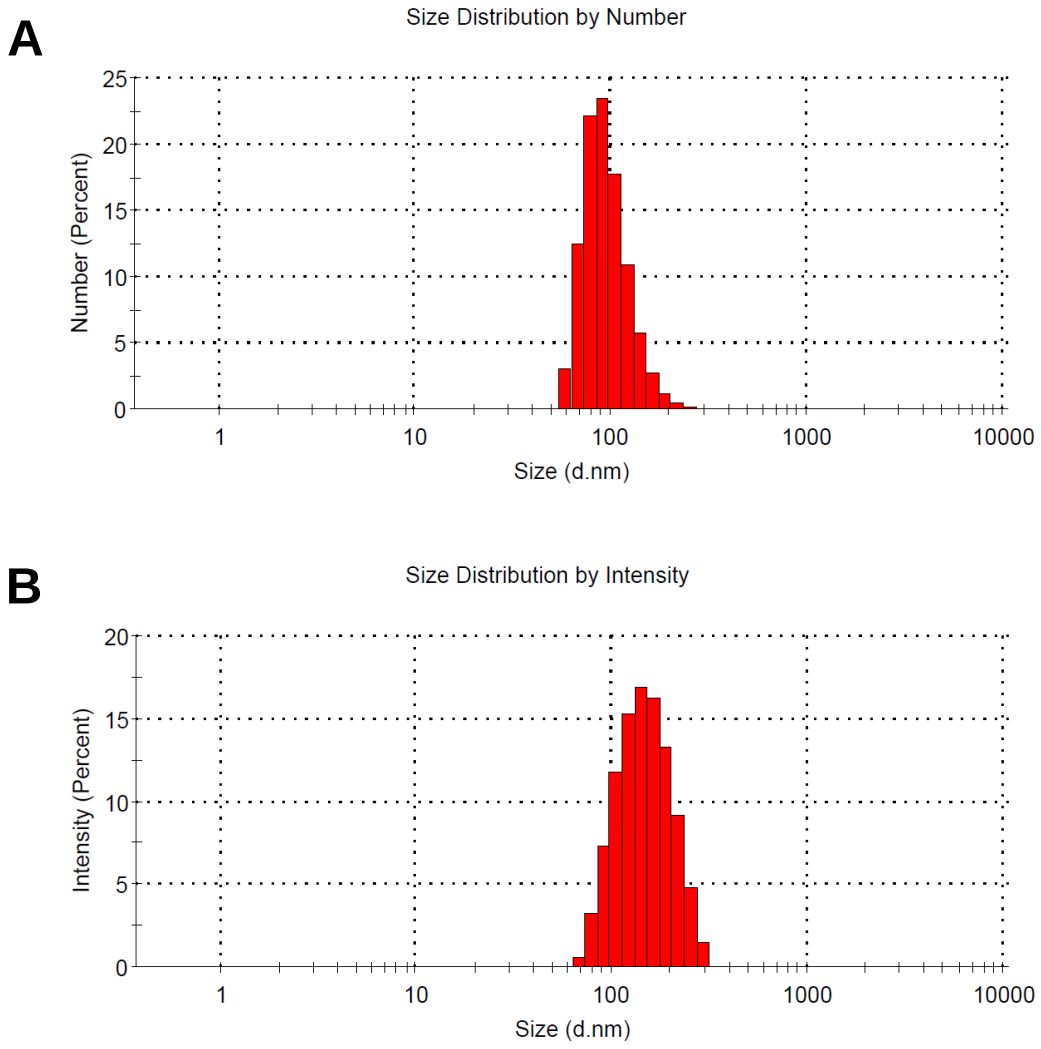

Supporting Figure S1. Size distribution of CD20/44-siNC-LbL-NPs calculated by **(A)** number and **(B)** intensity.

Supporting Table S6. Characterization of HA-TET, CD20-TCO and CD20-LbL-NPs

Sample	TET / HA [a]	TCO / Ab [b]	Ab / NP [c] (μg / mg)	siRNA / NP [d] (μg / mg)	Efficiency [e] (%)
HA-TET	16.1				51.0
CD20-TCO-NHS		5.2			26.0
CD20-TCO-Thio		4.1			20.5
CD20-TCO-NHS- LbL-NP			0.41		16.2
CD20-TCO-Thio- LbL-NP			0.37		14.5
siRNA-LbL-NP				124.0	4.1

[a] Number of methyltetrazine molecules conjugated to a hyaluronic acid, measured by a UV spectrometer.

[b] Number of TCO molecules conjugated to a CD20 antibody. TCO conjugation was quantified by a fluorescence spectrometer after Cy3-tetrazine molecules were conjugated to the TCO molecules on CD20-Ab.

[c] CD20 antibody (μg) per 1 mg of PLGA nanoparticles. The amount of CD20 was quantified by a fluorescence spectrometer using fluorescently labeled CD20 antibody

[d] siRNA (μg) per 1 mg of PLGA nanoparticle core. The amount of siRNA was quantified using a using Quant-iT™ RiboGreen® RNA Assay Kit.

[e] Conjugation/loading efficiency. Weight percentage of amount of TET, TCO, CD20-Ab or siRNA relative to the initially feeding amount.

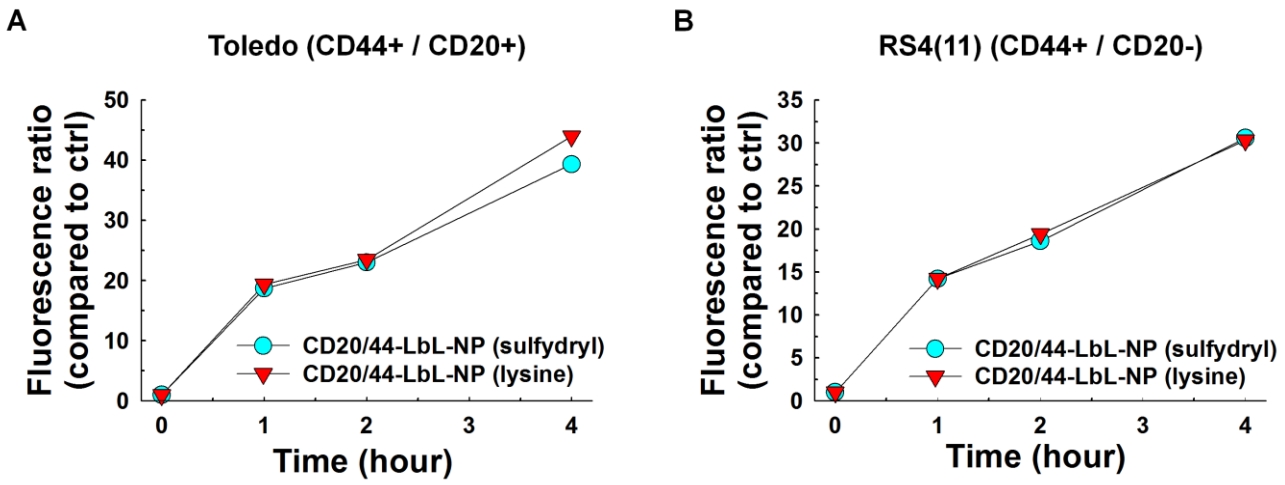

Supporting Figure S2. Relative fluorescence intensities of **(A)** Toledo and **(B)** RS4(11) cells treated with fluorescently labeled CD20/CD44 dual-targeted LbL-NPs prepared by lysine or sulfhydryl modification method.

Targeting blood cancer cells. The outer layer of hyaluronic acid-CD20 antibody conjugate was prepared via two different antibody conjugation methods—lysine modification and sulfhydryl modification—to figure out which approach led to more optimal conjugation (Supporting Scheme S1,2). FACS results indicated that sulfhydryl modified CD20/44-LbL-NPs showed 11.8% higher cellular uptake into Toledo cells at 4 h than lysine modified CD20/44-LbL-NPs, implying the sulfhydryl modification method affected the binding affinity of the anti-CD20 Ab less than lysine modification method. However, CD20/44-LbL-NPs (sulfhydryl) did not show significant increase in cellular uptake into the RS4(11) cells compared to CD20/44-LbL-NPs (lysine) indicating CD20-targeting is not the main cellular uptake mechanism for CD20-negative RS4(11) cells (Supporting Fig. S2).

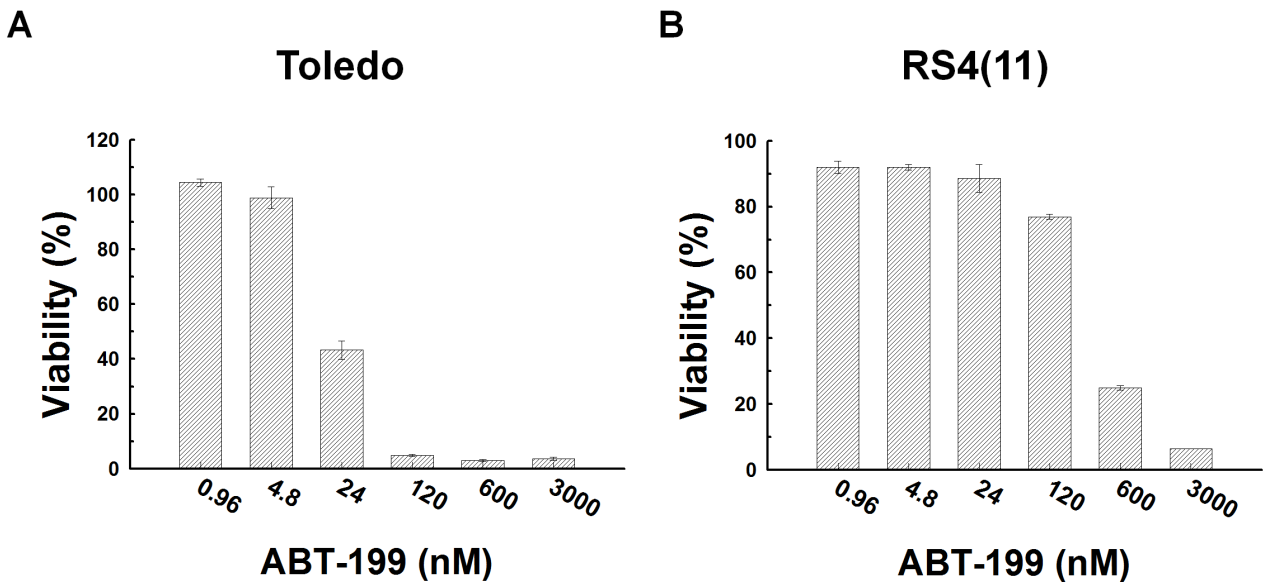

Supporting Figure S3. Cell viability of **(A)** RS4(11) and **(B,E)** Toledo cells after treatment with a small molecule BCL-2 inhibitor ABT-199.

BCL-2 dependent cell viability. To evaluate BCL-2 dependent cell viability of RS4(11) and Toledo cells, we treated the cells with a small molecule BCL-2 inhibitor, ABT-199 (Venclaxta™, Abbvie, Genentech). ABT-199 treatment decreased viability of RS4(11) and Toledo cells in a dose-dependent manner, implying that BCL-2 is a crucial protein that mediates between cell survival and death (Supporting Fig. S1).

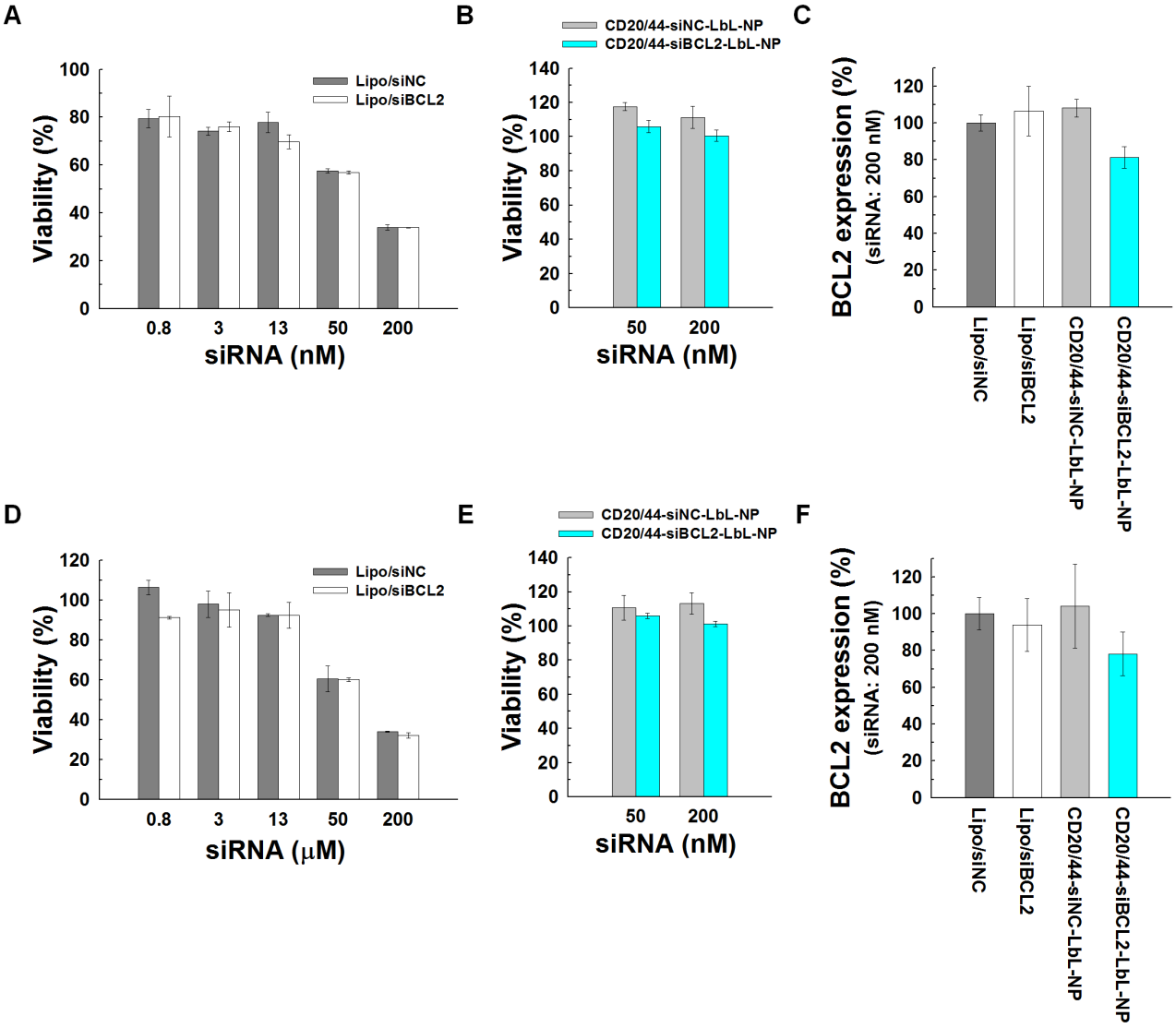

Supporting Figure S4. Cell viability of **(A,D)** RS4(11) and **(B,E)** Todedo cells after treatment with negative control siRNA cocktails (siNC) or BCL-2 target siRNA cocktails (siBCL2) formulated with Lipo or LbL-NPs (LNPs). BCL-2 expression on **(C)** RS4(11) or **(F)** Toledo cells after treatment with siNC or siBCL2.

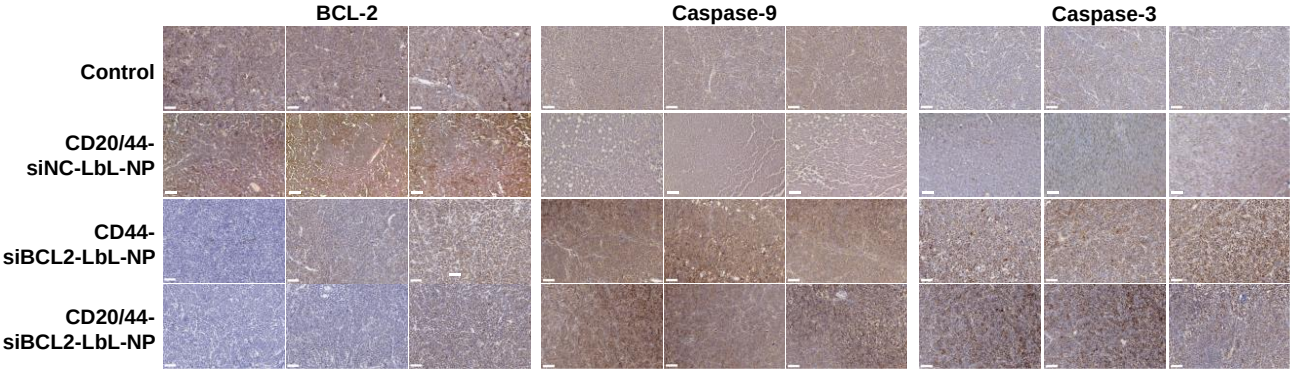

Supporting Figure S5. Immunohistochemistry images of tumor sections collected from SCID beige mice intravenously injected with Toledo cells and LbL-NPs (scale bar = 50 μm).

First, we evaluated changes in BCL-2 protein levels by a western blot. We lysed the tumor tissues and assessed BCL-2 expression levels in the tumor lysate. Western blot results showed significantly lower BCL-2 expression levels in the tumor lysates of CD44-siBCL2-LbL-NP and CD20/44-siBCL2-LbL-NP groups than those of the control group (Fig. 7a,c).

Supporting Table S7. Serum Levels of ALT, SAT, ALK and TP [a]

Assay	Normal	Units	CD20/44-siBCL2-LbL-NP	CD44-siBCL2-LbL-NP
Alanine Aminotransferase (ALT)	17~77	U/L	34 ± 0.71	41± 3.5
Aspartate Aminotransferase (AST)	54-298	U/L	104 ± 12.7	100 ± 24.0
Alkaline phosphatase (ALK)	35-96	U/L	64 ± 18	51 ± 13
Protein, Total (TP)	3.5-7.2	g/dL	6.2 ± 0.14	5.7 ± 0.14

[a] Data are mean ± SD (n=2 per goup).

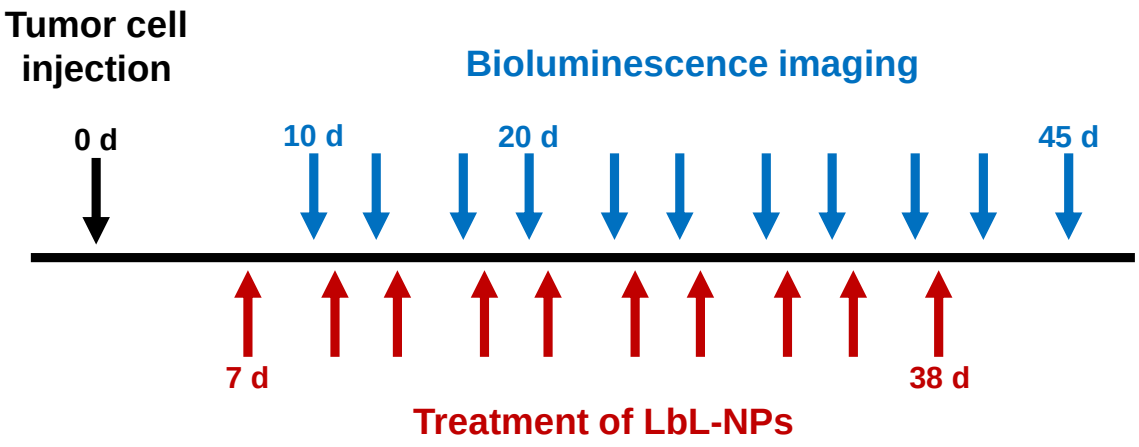

Supporting Figure S6. Diagram of the general procedure.